01 Jan 1990

Experimental And Theoretical Study Of The Electron Spectra In 66.7350-keV/u C++He Collisions

L. H. Toburen

R. (Robert) D. DuBois
Missouri University of Science and Technology, dubois@mst.edu

C. O. Reinhold

D. R. Schultz

et. al. For a complete list of authors, see https://scholarsmine.mst.edu/phys_facwork/2639

Recommended Citation

L. H. Toburen et al., "Experimental And Theoretical Study Of The Electron Spectra In 66.7350-keV/u C++He Collisions," *Physical Review A*, vol. 42, no. 9, pp. 5338 - 5347, American Physical Society, Jan 1990.
The definitive version is available at https://doi.org/10.1103/PhysRevA.42.5338

Experimental and theoretical study of the electron spectra in 66.7–350-keV/u $C^+ + He$ collisions

L. H. Toburen and R. D. DuBois
Pacific Northwest Laboratory, Richland, Washington 99352

C. O. Reinhold, D. R. Schultz, and R. E. Olson
Department of Physics, University of Missouri-Rolla, Rolla, Missouri 65401
(Received 28 June 1990)

Measurements of the differential and total cross sections for production of free electrons are reported for collisions of 66.7–350-keV/u C^+ ions with He. The experimental data are compared with theoretical calculations that include electron emission from both target and projectile using the classical-trajectory Monte Carlo method and the independent-electron approximation. Good agreement is observed between theory and experiment, and structures appearing in the electron spectra can be explained in terms of either, or both, target and projectile ionization.

I. INTRODUCTION

Ionization of atoms and molecules produced by collisions with fast charged particles plays an important role in such diverse fields as fusion energy, atmospheric and astrophysical sciences, and radiation biology. Study of the energy and angular distributions of electrons ejected in these ionizing collisions provides detailed information on the interaction mechanisms. An extensive literature has been established regarding the cross sections for electron emission by light ion impact; see, for example, reviews by Toburen,[1] Berényi,[2] Stolterfoht,[3] and Rudd.[4]

Although the first measurements of the ejected-electron spectra resulting from bare-ion impact were conducted more than 25 years ago, the theoretical understanding of these collisions is still progressing. For high impact velocities (v) and small projectile charges (Z_p) the electron spectra are found to be well described, except for very small ejection angles, by the first Born approximation for direct ionization.[5,6] More specifically, the first Born approximation provides reasonably good results when $(v/v_0)/Z_p \gg 1$ a.u., v_0 being the initial orbital velocity of the target electron. When this condition is not satisfied, the first Born approximation fails in accurately predicting the angular distributions of the ionized electrons. Under such conditions, it is necessary to resort to more elaborated theoretical models which go beyond first-order approximations and describe ionized electrons as electrons in the continuum of the combined target-nucleus–projectile Coulomb field (i.e., so-called two-center treatments).[7–12] So far, theoretical models such as distorted-wave approximations[7–9] or classical-trajectory Monte Carlo (CTMC) methods[11,12] have successfully been utilized for bare ions with impact velocities as low as $(v/v_0)/Z_p = 1$ a.u.

Our theoretical understanding of collisional ionization involving ions that carry bound electrons (clothed ions), or neutral projectiles, is at a much more primitive stage of development, even though the first measurements of doubly differential cross sections for electron emission for clothed-ion impact were conducted more than 20 years ago.[13,14] The basic features of the electron spectra resulting from interactions of high-energy clothed ions with atomic and molecular targets were first identified in work by Wilson and Toburen,[15] Burch, Wieman, and Ingalls,[16] and Stolterfoht *et al.*[17]

In general, there has been a lack of theoretical studies that consider electron emission from both target and projectile at intermediate impact energies [i.e., $(v/v_0)/Z_p \sim 1$ a.u.]. At high impact energies and for collision systems involving He^+ projectiles and noble gas targets, calculations using the first Born approximation have been reasonably successful.[18–20] Similar calculations, however, have not been conducted for more complex ions. At low impact energies [i.e., $(v/v_0)/Z_p < 1$ a.u.], experimental data have been interpreted in terms of molecular promotion models.[21–23] These models provide qualitative information about the shape of the spectra of ejected electrons, but little information regarding the absolute magnitudes of the cross sections.

In this work, we extend the two-center CTMC technique to include both target and projectile electron emission within the independent-electron approximation.[24] The results obtained with this model are compared to present experimental measurements of the electron-emission cross sections arising from collisions of 66.7–350-keV/u C^+ ions with helium atoms (i.e., $0.97 < v/v_0 < 2.21$).

II. EXPERIMENTAL TECHNIQUE

A. Apparatus

The energy and angular distributions of electrons ejected in $C^+ + He$ collisions were measured for ions in the energy range 66.7–350 keV/u. The electron energy spectra were obtained using an electrostatic energy analyzer that could be positioned at electron-emission angles from 15° to 130°. The experimental technique used in this work was described previously for studies of electrons emitted in low-energy proton collisions[25] and will be only briefly discussed here. For the present studies carbon ions were

obtained using a 2-MV tandem electrostatic accelerator injected with negative ions from a sputter source. Gas stripping was employed in the accelerator high-voltage terminal to convert the negative ions to positive ions for the second acceleration stage. After acceleration, ions were magnetically analyzed for charge and energy before entering the collision chamber through a series of collimators. The entrance collimation system included a biased collimator for suppression of electrons formed in ion-beam slit-edge scattering. The beam transport system was pumped to approximately 10^{-7} torr to reduce the probability of charge transfer from interactions of the ion beam with residual gas atoms. This, plus the relatively short path length through the target gas, served to minimize charge-state contamination in the transmitted beam. That no corrections for charge-state contamination were required was confirmed by yield measurements in which the path length for ion transport was reduced by approximately a factor of 2 with no change in the derived cross sections.

A schematic drawing of the apparatus used in the measurements is reproduced in Fig. 1. The collimated, energy and charge selected, ion beam was passed through a diffuse atomic helium beam and collected in a shielded, biased Faraday cup. The atomic beam target was produced by diffusion of helium gas through a microchannel plate. The microchannel plate was approximately 1 cm in diameter, 1 mm in thickness, and contained channels with a length-to-diameter ratio of 100. Helium gas was introduced above the microchannel plate at a pressure of 1 torr maintained by monitoring with a capacitance manometer that provided feedback control to a motor driven gas inlet valve.

Electrons ejected in ion-atom collisions were energy analyzed by a cylindrical mirror electrostatic energy analyzer and detected by a continuous channel electron multiplier. The detection efficiency of the electron multiplier for electrons with energies from 15 to 600 eV was taken as 99% followed by a linear decrease to 75% at 2200 eV.[26] The solid angle subtended by the analyzer collimation was approximately 10^{-4} sr. The voltage on the electrostatic analyzer was controlled by an on-line computer which also recorded the electron yield for a preset number of collected ions.

Magnetic fields in the vicinity of the interaction region were reduced by housing the entire collision chamber in a double-walled magnetic shield. This shield and a set of Helmholtz coils reduced the magnetic fields to less than a few mG in the collision region. Stray electric fields from static charge buildup and/or variations in surface potentials were reduced by coating exposed surfaces with colloidal graphite.

An example of the raw data obtained for electron yields as a function of ejected-electron energy is shown in Fig. 2. This display of the number of electrons detected at a given energy per 6.2×10^{11} transmitted carbon ions shows the rapid decrease in electron yield with increasing emission angles. Plotted in this manner the electron yield

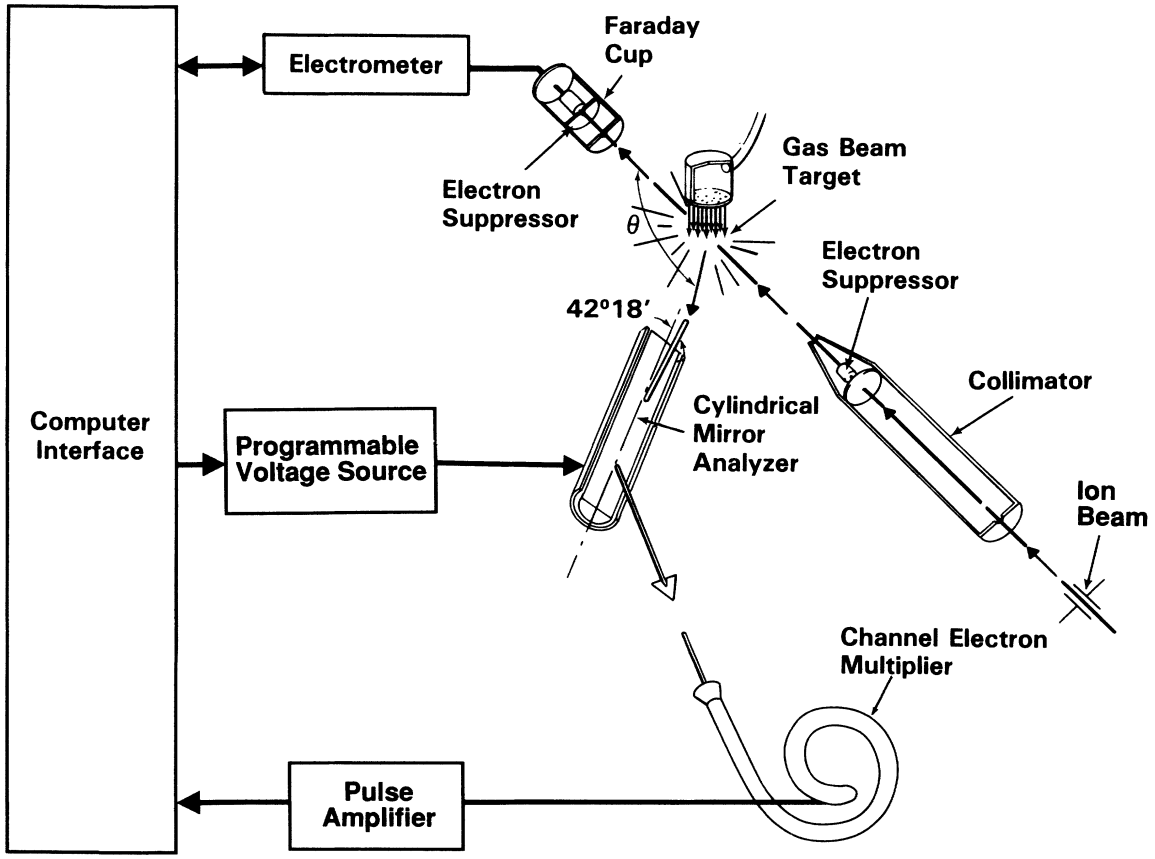

FIG. 1. Schematic drawing of the experimental system.

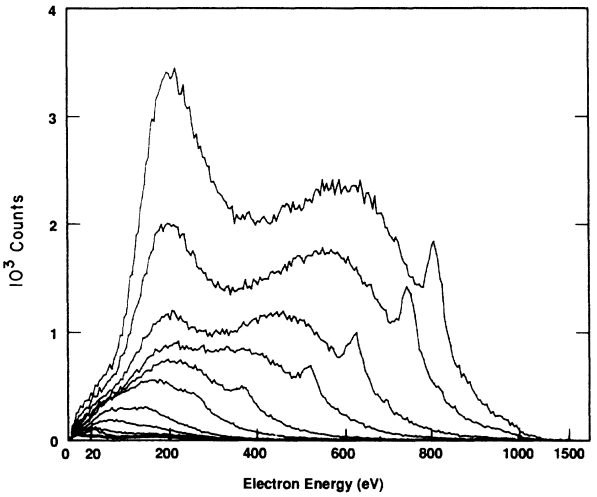

FIG. 2. Yield of electrons for 6.2×10^{11} ions per energy point as a function of electron energy. The vertical axis is proportional to the product of electron energy and emission cross section. The largest yield is for electron emission into 15°. Decreasing yields represent electrons emitted at angles of 20°, 30°, . . . , 130°.

is proportional to the emission cross section multiplied by the transmitted electron energy (the transmission of an electrostatic analyzer is proportional to the electron energy), which clearly illustrates three of the basic features of the emission spectra. The peak at approximately 180 eV (the energy scale is nonlinear at the lowest, $E<20$ eV, and highest, $E>900$ eV, energies) results from ionization of the incident carbon ion. Owing to the kinematics of the ionization process in the projectile frame of reference and the transformation to the laboratory reference frame these electrons are observed at approximately the same energy for all emission angles and form the "electron loss to the continuum" (ELC) ridge.

The second peak, occurring at about 600 eV in the 15° spectrum and at smaller energies for larger angles, is the "binary encounter" peak associated with electrons ejected by direct collisions between the carbon ion and electrons of the helium atom. This peak is observed at smaller electron energies as the emission angle is increased, obeying the classical kinematic scattering relationships, i.e., Rutherford scattering of the carbon ion from a "free" electron. The peaks at the upper end of the spectra result from Auger electron emission following collisionally induced K-shell vacancy production in the carbon projectile. The energy of the Auger transitions is Doppler shifted to higher energies when observed in the laboratory owing to the projectile velocity. The data shown in Fig. 2 were all normalized to 6.2×10^{11} C^+ ions per channel for comparison of relative yields. In practice, data for the larger angles, where yields are small, were accumulated for greater numbers of transmitted ions in order to obtain adequate statistics for reliable cross-section analysis.

B. Data analysis

The use of an atomic beam target in this work makes direct conversion of the yield measurements to absolute cross sections based on experimental parameters impractical because the target density profiles are unknown. Therefore, to place the relative yields on an absolute basis, separate measurements were made using the present directed gas target for 1.5-MeV protons where previously published absolute cross sections were available.[27] These data were used to obtain a calibration factor relating the relative electron yield to the absolute cross sections under experimental conditions identical to the carbon-ion measurements. In principle, it is necessary to obtain calibration factors for each angle investigated because the path length of the ion beam and the gas density viewed by the collimated electrostatic analyzer vary with electron-emission angle. In the present work the angular response of the system was determined from measurements of the intensity of the K Auger electrons emitted in proton excitation of the K shell of molecular nitrogen; these Auger electrons were assumed to be emitted isotropically. Calibration spectra for $H^+ + He$ collisions taken at several angles were in excellent agreement with the angular distributions derived from the Auger measurements.

To provide confidence that the calibration constants chosen to place the relative electron yields on an absolute scale were appropriate, the derived cross sections were compared to independent measurements of both total electron-emission cross sections and carbon K-shell ionization cross sections. Total electron-emission cross sections were obtained from coincidence measurements made in our laboratory for the yield of target ions produced by direct and charge-transfer ionization involving charged particles in the energy range from a few hundred keV to 2 MeV; the experimental technique has been described by DuBois.[28,29] Such data provide a measure of the total yield of electrons emitted in ionizing collisions by summing the number of electrons released in each collision channel. Data have been obtained for 0.36-, 0.7-, and 1.4-MeV N^+ ions in which total cross sections for single and double ionization of helium were measured for direct ionization, electron capture plus target ionization, and single and double electron loss from the projectile simultaneous with target ionization. Similar data are available for direct ionization and capture plus ionization by C^+ ions with energies of 0.4, 0.9, and 1.8 MeV. Using the N^+ results as a guide, we have estimated the projectile electron-loss contribution to the total electron production cross sections for C^+ ions. Total electron production cross sections derived from these measurements are compared to total electron production cross sections obtained by integration of the doubly differential data in Fig. 3 and in Table I. Excellent agreement is observed between the different methods of obtaining the total yields. Error bars reflect the estimated uncertainties associated with the various assumptions made in the analysis. In the analysis of electron yields based on coincidence measurements the contributions from ionization of the projectile leaving the target in the ground or excited, but not ionized, state were not included; this experimental technique that extracts target ions is not amenable to the study of that interaction channel. If one assumes that the electron contribution from this channel is

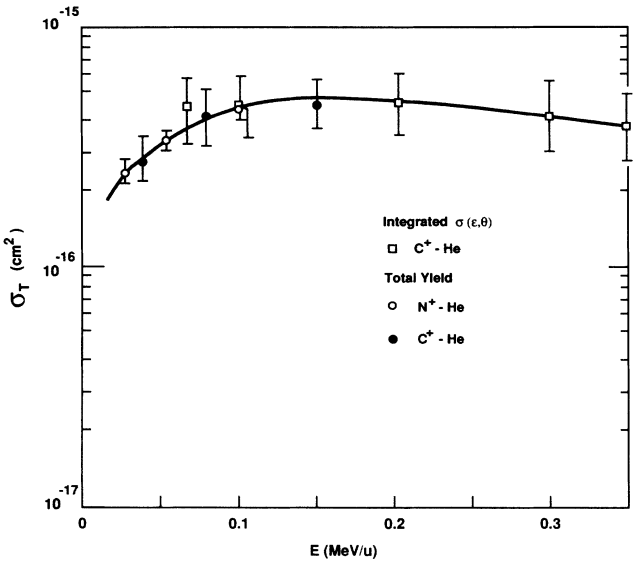

FIG. 3. Total cross sections for the production of electrons in collisions of C^+ and N^+ ions with helium. Cross sections obtained by integration of measured doubly differential cross sections are compared with those obtained from coincidence measurements of total ion yields.

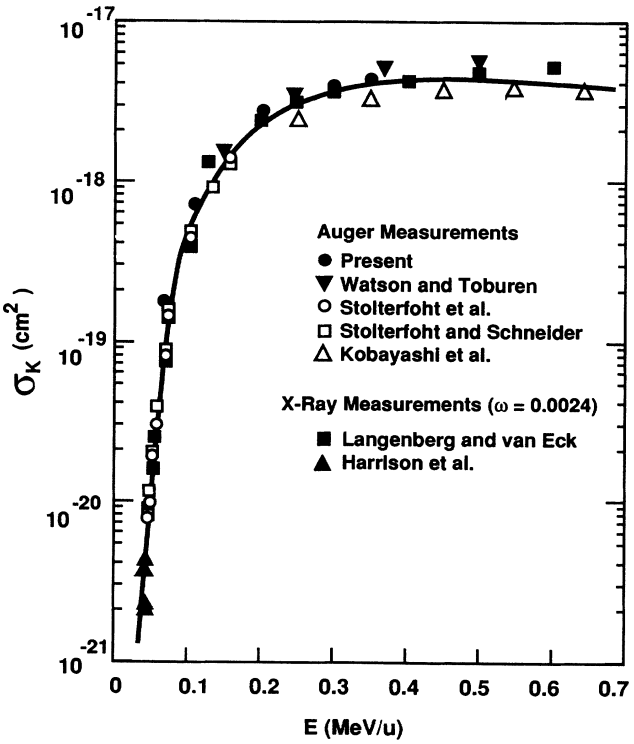

FIG. 4. Carbon K-shell ionization cross sections for $C^+ + He$ collisions compared with previous measurements for He^+ and He^{2+} collisions with carbon targets. The previously published data are from (▼) Watson and Toburen (Ref. 30), (○) Stolterfoht *et al.* (Ref. 31), (□) Stolterfoht and Schneider (Ref. 32), (△) Kobayashi *et al.* (Ref. 33), (■) Langenberg and van Eck (Ref. 34), and (▲) Harrison *et al.* (Ref. 35).

as large as that due to projectile electron loss plus target ionization, which was measured, the total electron yield would be increased by approximately 10%; we feel this assumption is, however, an overestimation for that electron production channel.

The emission of K Auger electrons from the projectile, illustrated by the peaks superimposed on the high-energy end of the continuum spectra in Fig. 2, provides another meas to assess the reliability of the absolute values of the doubly differential cross sections. The absolute cross sections for Auger emission were obtained from the doubly differential cross sections by first fitting a third-order polynomial to the continuum spectra above and below the energy of the Auger transitions to estimate the continuum "background" on which the Auger spectra are superimposed. This background was then subtracted and the resulting Auger spectrum integrated to obtain the singly differential, angular-dependent, Auger emission cross section. Conversion of the energy and intensity of the Auger cross sections from the laboratory rest frame to the projectile frame was performed as described by Stolterfoht[3] and the total cross section for Auger emission was obtained assuming emission to be isotropic in the emitter rest frame. The total cross section obtained from these data is compared with previously published data for inner-shell ionization of carbon by helium ions based on Auger electron[30–33] and x-ray[34,35] yield measurements in Fig. 4. For comparison, the x-ray measure-

TABLE I. Total cross sections for production of free electrons in units of 10^{-16} cm^2.

E (kev/u)	Theory $C^+(2s^2,2p)$	Theory $He(1s^2)$	Expt.[a] $He(1s^2)$	Theory total	Expt. total[b]	Expt. total[c]
33.33			2.14		2.89	
66.66	1.35	1.96		3.31		4.7
75			2.96		4.16	
100	1.19	2.36		3.55		4.8
150			2.77		4.46	
200	0.87	2.59		3.46		4.7
300	0.73	2.35		3.08		4.2
350	0.68	2.25		2.92		3.8

[a]From DuBois and Toburen (Ref. 52).
[b]From coincidence measurements of total ion yields.
[c]From integrated doubly differential electron-emission cross sections.

ments were converted to ionization cross sections using the fluorescence yield of 2.4×20^{-3} given by Langenberg and van Eck;[34] this fluorescence yield is also in close agreement with recent calculations of Hartmann.[36] The excellent agreement of the present measurements with previously published results lends confidence to our absolute calibration.

III. THEORETICAL TECHNIQUE

The classical-trajectory Monte Carlo treatment of ion-atom collisions involving one active electron has been described fully by Abrines and Percival,[37] Olson and Salop,[38] and others. Given an initial approximated phase-space state for the target and the projectile, the major assumption that is made in this method is that the evolution of this state can be calculated by means of classical mechanics. The initial state for the projectile is chosen so as to represent a uniform flux of impinging particles with well-defined momentum. In addition, the initial state for the target is chosen so as to approximate the quantum-mechanical momentum and position probability densities of the bound electron. Usually, this is accomplished by means of the microcanonical ensemble introduced by Abrines and Percival[37] which reproduces exactly the quantum-mechanical momentum distribution of a hydrogenic target.

For bare-ion impact of hydrogenic targets no other assumptions are made since the electron–target-nucleus and electron-projectile interactions are exactly taken into account. However, additional approximations must be made to study collisions involving many active electrons. These approximations typically consist of using the independent-electron approximation[24] and, therefore, representing the electron-electron interactions by means of static central potentials. The earliest type of potential that has been considered is the screened Coulomb interaction.[38–41] Extension of the CTMC formalism to consider structured projectiles by means of more general interactions which have the correct behavior at small and large distances presents no difficulty and has recently been accomplished by McDowell and Janev[42] and Reinhold and Schultz.[43] However, to treat many-electron targets subject to non-Coulomb interactions, an alternate method to the one proposed by Abrines and Percival[37] for Coulomb potentials had to be developed to sample initial electronic conditions. Recently, an approximation method has been developed by Peach *et al.*[44] and different, simpler methods have been proposed by Reinhold and Falcón[45] and Cohen and Fiorentini.[46]

In order to obtain doubly differential cross sections with reasonably small statistical uncertainties by means of the CTMC technique, a very large computational effort is required. Nevertheless, the first calculations were performed in 1971 by Bonsen and Banks[39] for collisions of protons with helium, but no other comparable study of doubly differential cross sections using this technique followed for more than ten years. With the recent widespread availability of supercomputers, several other studies have been performed (see Refs. 11, 12, 43, 47, 48, and references therein), and works such as the present one have become feasible.

Previous CTMC calculations of the ejected-electron spectra arising from clothed-ion–atom collisions have only considered the possibility of target electron emission. In this work, we extend these studies to consider electron emission from both target and projectile. To this end, electron-electron interactions are approximated by using the model potentials derived by Garvey *et al.*[49] by a variational procedure in a modified Thomas-Fermi model. This kind of interaction has previously and successfully been used for bare-ion–atom collisions using the CTMC method.[50]

Thus it is assumed that each electron interacts simultaneously with a target (t) core and a projectile (p) core through the two-center potential

$$V(r)=V_t(r_t)+V_p(r_p) \tag{1}$$

with

$$V_{t,p}(r)=\frac{1}{r}[N_{t,p}S_{t,p}(r)-Z_{t,p}] \tag{2}$$

and

$$S_{t,p}(r)=1-[(\eta_{t,p}/\xi_{t,p})(e^{\xi_{t,p}r}-1)+1]^{-1}\ , \tag{3}$$

where $Z_{t,p}$ and $N_{t,p}$ denote the nuclear charge and number of nonactive electrons in the target core and the projectile core, respectively, and $\eta_{t,p}$ and $\xi_{t,p}$ are the screening parameters derived by Garvey *et al.*,[49] depending on $N_{t,p}$ and $Z_{t,p}$. A brief comment about this model with special attention to forward electron emission has already been made in a previous article.[51]

As a first test for the model, we have studied the $C^+ + He$ collision system assuming that the electrons in the K shell of C^+ do not play a significant role; i.e., only the $1s^2$ electrons of helium and the $2s^2,2p$ electrons of C^+ have been taken into account in the calculations. The initial $He(1s^2)$ and $C^+(2s^2,2p)$ electronic configurations have been represented by microcanonical ensembles with binding energies of -0.904 a.u. (experimental ionization potential of He) and -1.07 a.u. (weighted average of the Hartree-Fock orbital energies of the $2s$ and $2p$ sublevels of C^+).

The resulting model accounts for electron removal from both projectile and target and includes simultaneously electron capture, ionization, and excitation for each center. In principle, the Hamiltonian equations for all the electrons can be solved simultaneously. In practice, an equivalent result is obtained from the combination of two three-body calculations. In the first calculation the three bodies are the projectile (C^+), target core (He^+), and target electron (e) with the appropriate model potentials (C^+-e, He^+-e, C^+-He^+). In the second, they are the projectile core (C^{2+}), projectile electron (e), and target (He^0) with the corresponding interactions (C^{2+}-e, He^0-e, C^{2+}-He^0). The results of the two calculations are then summed to obtain the gross electron-emission cross sections, or may be combined using the independent-electron model to yield cross sections dependent on the coincident charge states of the target and projectile.

As with any theoretical approximation, it is difficult to assess precisely the valid range of the model. According to our experience, we expect this model to give reasonably good results for the $C^+ + He$ collision system in the impact energy range $70 \leq E \leq 1200$ keV/u. However, as the present CTMC model contains additional approximations, the major new approximation being the representation of the target-electron–projectile-electron interactions by central model potentials, the strict limits of validity must be determined by comparison with experiment.

IV. RESULTS AND DISCUSSION

To illustrate the general features of the electronic spectra, we display in Fig. 5 the theoretical and experimental doubly differential cross section for electron emission in collisions of 350-keV/u C^+ ions with helium at selected ejection angles from 1° to 140°. The basic structures of the experimental ejected-electron spectra are well reproduced by the present CTMC calculations. The most obvious difference between the calculated and measured spectra appears to be the enhancement in the experimental cross sections at low electron energies and large emission angles. Auger structures observed on the experimental spectra are not seen in the calculated spectra as K-shell ionization of carbon is not presently included in the calculation.

In order to identify the origin of the structures appearing in the electron spectra, it is very useful to separate the total yield of electrons into its different components. Within the present independent-electron model, it would be possible to separate the spectra into the yield of electrons associated with each different final partition, including simultaneous single and multiple ionization, excitation, and electron capture for each center. However, a more illustrative separation of the spectra for our purposes here is to divide it into target electron emission and projectile electron emission. Because of the indistinguishability of the electrons, this kind of separation is not feasible experimentally.

In Fig. 6 we display the separation of the electron spectra of Fig. 5 into target electron emission and projectile electron emission. We first note that the basic structures appearing in the total yield of electrons clearly arise from either, or both, target and projectile ionization. For example, at large ejection angles both theory and experiment display a shoulder in the total yield at an electron energy of approximately 190 eV, corresponding to electrons ejected with velocities close to the projectile velocity v (this electron energy will be denoted by E_p and is given by $E_p = 0.5v^2$ a.u.). Separation of the spectra into target (He) and projectile (C^+) electron emission indicates that the shoulder is due to the yield of electrons arising from the ionization of C^+.

Furthermore, as can be seen in Fig. 6, the electron

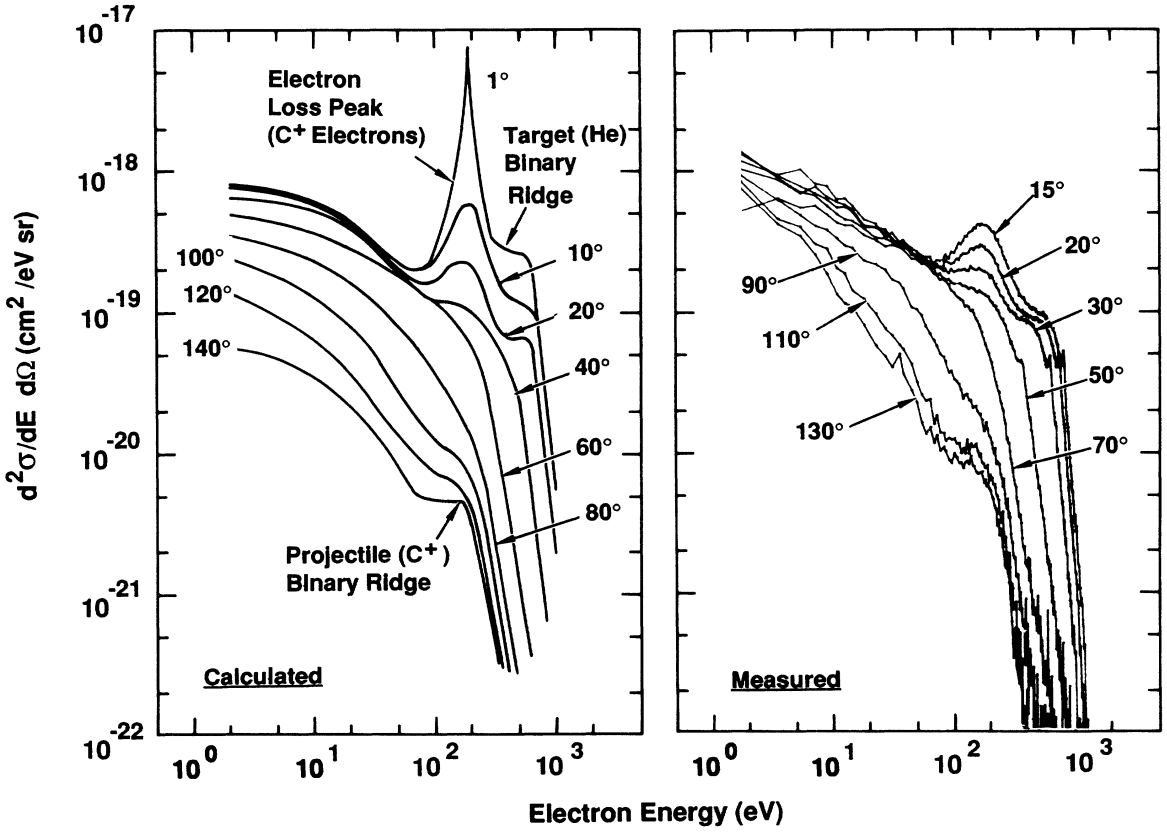

FIG. 5. Doubly differential cross sections for electron emission in 350-keV/u C^+-He collisions calculated with the CTMC method (left panel) and measured (right panel).

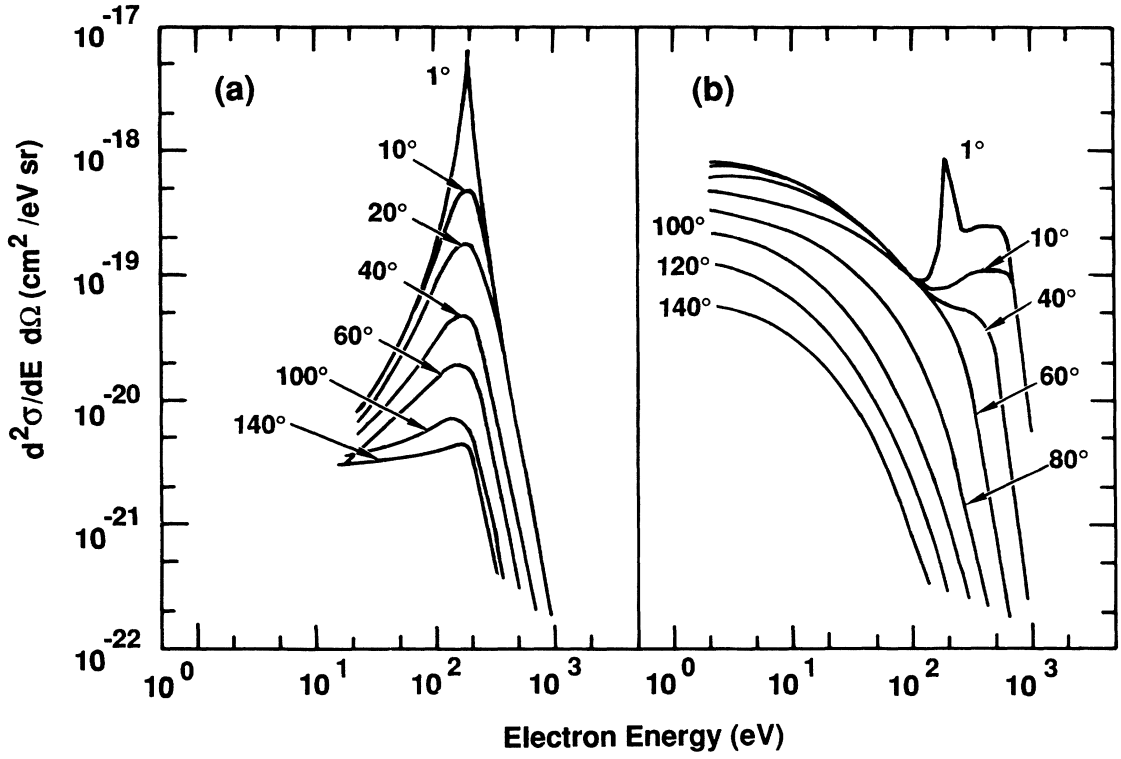

FIG. 6. The theoretical doubly differential cross section of Fig. 5 is separated into cross sections for projectile electron emission (left panel) and target electron emission (right panel).

spectra arising from projectile ionization display a peak at electron energies close to E_p almost independent of ejection angle, forming a ridge. This structure is usually referred to as the electron loss to the continuum (ELC) peak and becomes a very sharp cusplike feature at very small ejection angles. Analysis of the dynamics of the collision indicates that the origins of the backward and the forward ELC peaks are very different in nature. That is, while the forward ELC peak is due to electron emission in soft collisions, the backward ELC peak arises from a binary collision between projectile electrons and the target core. In other words, the backward ELC peak is the well-known binary peak associated with projectile ionization transformed to the target reference frame.[51]

Indeed, at small ejection angles (e.g., 15°–40°), separation of the electron-emission spectra into target and projectile ionization indicates that the forward peak at E_p is precisely the ELC peak. In addition, at higher ejection energies, the total yield exhibits a shoulder structure, which is the well-known binary peak for target electron emission. This feature is found at an energy of approximately $E_b = 2v_p^2\cos^2\theta - U_i$, where θ and U_i are the ejection angle and the ionization potential, respectively.

At very small ejection angles (e.g., 10°) another structure arising from target electron emission becomes increasingly important. This structure is the electron capture to the continuum (ECC) peak, which is formed when electrons removed from the target at very small emission angles are focused by the Coulomb field of the projectile in the asymptotic escape (e.g., see Ref. 12 and references therein). However, at an impact energy of 350 keV/u this peak is much smaller than the ELC peak. In contrast, we have observed that this situation is reversed at smaller impact energies, owing to the changing relative magnitudes of ionization and capture as a function of collision energy.[51]

Quantitative comparisons between theory and experiment can be made for total, singly differential, and doubly differential cross sections for free-electron production. Total cross sections are presented in Table I for electron emission from the target and from the projectile, as well as the sum. As was shown in Fig. 3, the integrated doubly differential cross sections and the total cross sections derived from coincidence measurements are in good agreement within the combined experimental uncertainties. These measurements are, however, consistently larger than the calculated total electron yield with the largest differences being at the larger ion energies. A comparison between calculated and measured target ionization[52] shows a similar discrepancy with the measured cross sections being about 20–30 % larger than calculated values. Thus the theory seems to underestimate both target and projectile total ionization by a similar amount.

We also note that total single-ionization cross sections for $C^+ + He$ (i.e., for the process $C^+ + He \rightarrow C^+ + He^+ + e$) have also been reported recently by

Janev, Phaneuf, and Hunter.[53] These cross sections are approximately a factor of 2.5 smaller than the single-ionization cross sections measured by DuBois and Toburen,[52] and are smaller than the present CTMC results as well.

Further insight into the origin of the differences between the present theoretical and experimental results can be obtained from a comparison of the ejected-electron spectra. Thus the calculated singly differential cross sections are compared, in Fig. 7, to the measured values obtained from integration of the doubly differential cross sections with respect to the emission angle. In general, the agreement between theory and experiment is remarkable in both spectral shape and absolute value. The largest discrepancies occur for low-energy electrons where the measured values are somewhat larger than those calculated. One must be cautious, however, in drawing conclusions for electron energies less than about 15 eV owing to the increased experimental uncertainties for these low-energy cross sections.

Similarly, a comparison of the calculated and measured angular dependence of all electrons emitted in C^+ collisions with helium is made in Fig. 8 where we display those singly differential cross sections as a function of the ejection angle. Again, the theoretical calculations are in good agreement with the experimental measurements as to the shape of the cross sections. However, discrepancies in the magnitude of the cross sections can be seen for ejection angles greater than about 50°.

A more detailed comparison of the theoretical results and the experimental data is made in Figs. 9 and 10, where we display the doubly differential electron-emission spectra at different ejection angles in 100- and 350-keV/u $C^+ + He$ collisions, respectively. Excellent agreement is observed between theory and experiment at an ejection angle of 20°. Furthermore, at an impact energy of 350 keV/u theory and experiment each exhibit clear evidence of electron emission from both target and projectile. On the other hand, there is little structure in the spectra for an impact energy of 100 keV/u to enable identification of the origin of emitted electrons. For this ion energy the projectile electron loss peak (ELC) should be centered at approximately 55 eV. However, on the basis of our calculations we conclude that the lack of a peak is due to (i) the decreasing influence of electron emission from the projectile at small ejection angles for this low ion energy and (ii) the fact that the width of the ELC peak is broad and, therefore, is smoothly merged with the target continuum.

At the larger ejection angles of 70° and 120°, good agreement between theory and experiment is only obtained for the high-energy portion of the spectra. This reflects the observation made above in the discussion of Fig. 5, that the measured cross sections at large angles

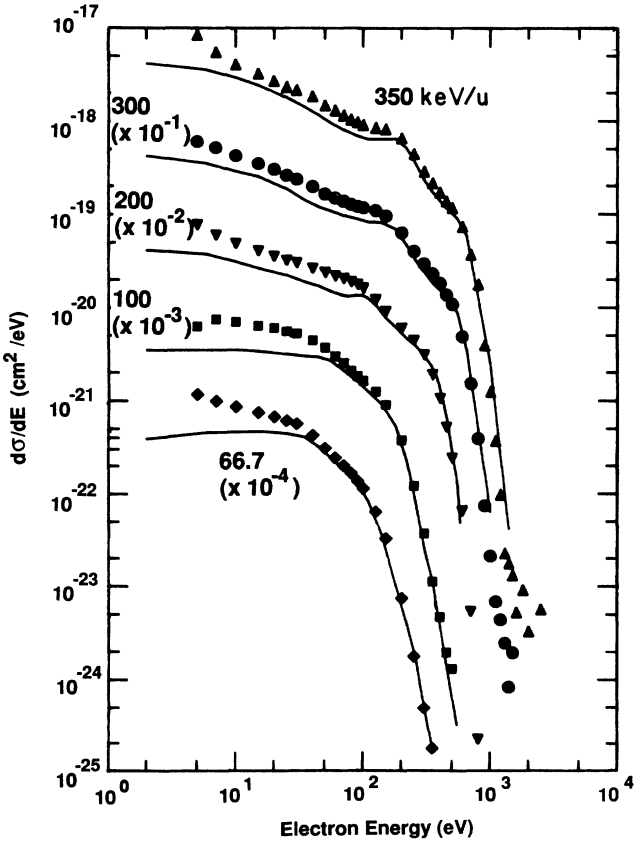

FIG. 7. Singly differential cross sections for electron emission as a function of the electron energy in C^+ collision with He at several impact energies. The solid lines and the symbols are the calculated and measured cross sections, respectively.

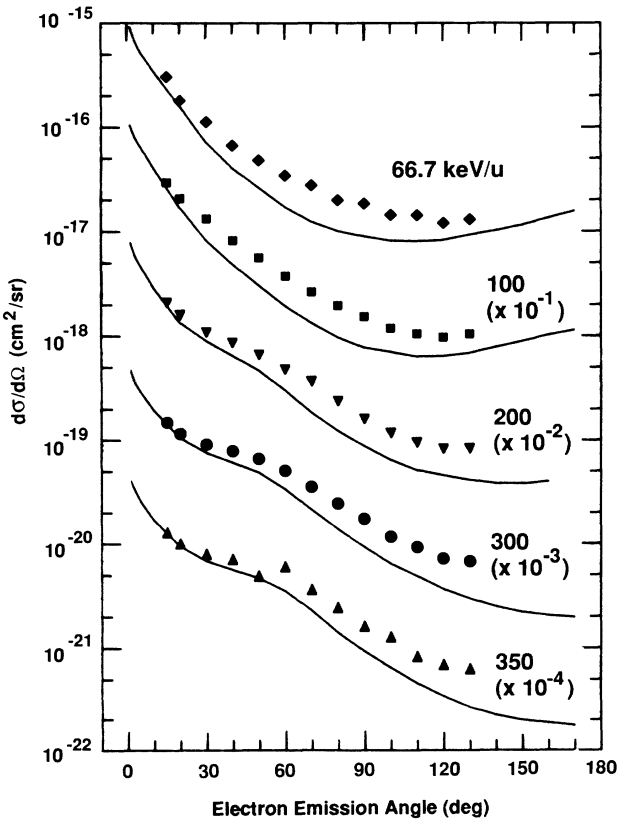

FIG. 8. Singly differential cross sections for electron emission as a function of the ejection angle in C^+ collisions with He at several impact energies. The solid lines and the symbols are the calculated and measured cross sections, respectively.

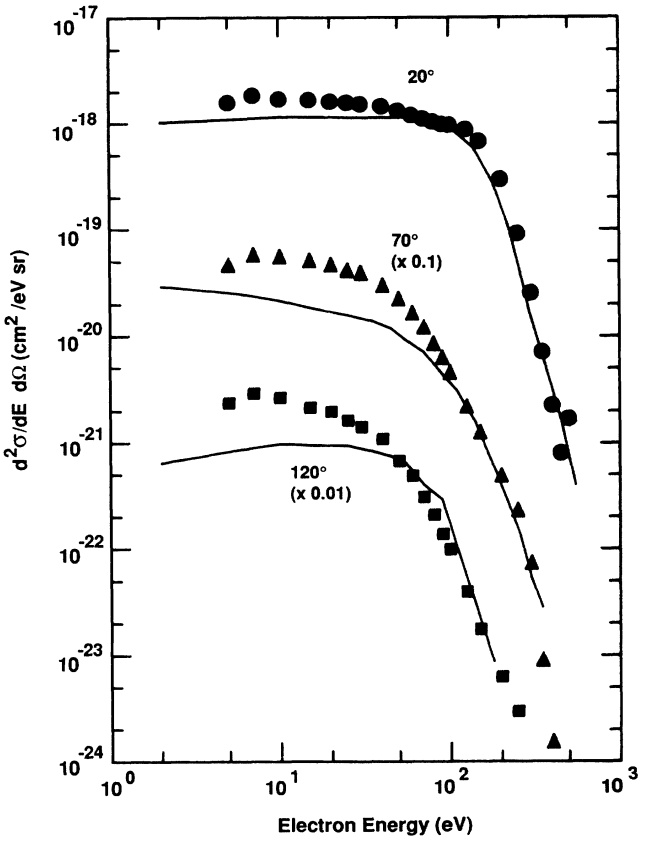

FIG. 9. Doubly differential cross sections for electron emission in collisions of 100-keV/u C^+ ions with helium at ejection angles of 20°, 70°, and 120° and as a function of the electron energy. The solid lines and the symbols are the calculated and measured cross sections, respectively.

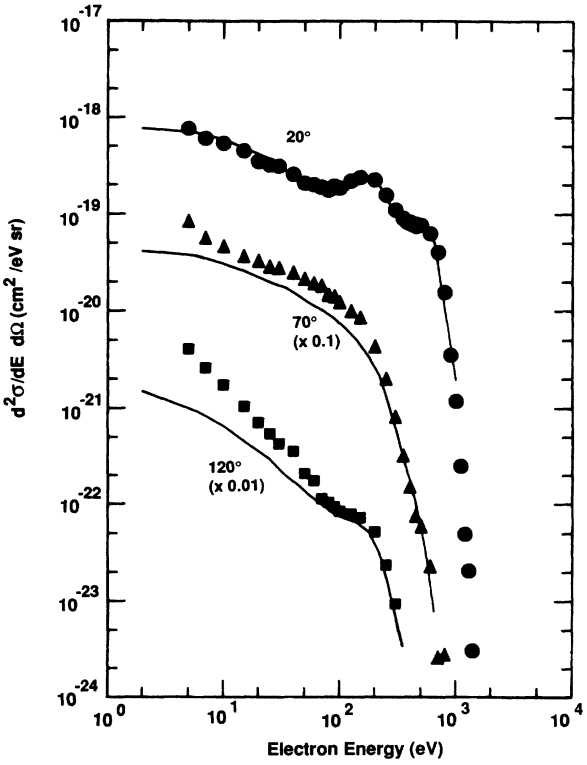

FIG. 10. Doubly differential cross sections for electron emission in collisions of 350-keV/u C^+ ions with helium at ejection angles of 20°, 70°, and 120° and as a function of the electron energy. The solid lines and the symbols are the calculated and measured cross sections, respectively.

tend to increase with decreasing electron energy faster than the calculated spectra. This discrepancy between theory and experiment may indicate a limitation in the description of electron emission at backward angles by means of the present CTMC model. Regarding experiment, improper background subtraction or the nature of the electrostatic analysis (which is often unreliable for electron energies below 15 eV) could result in an overestimation of the yield of electrons.

V. SUMMARY

An experimental and theoretical study has been conducted of the differential and total ionization cross sections for 66.7–350-keV/u C^+ ions colliding with helium atoms. Spectral features were identified as being related to projectile or target electron emission.

Differential cross sections calculated with the classical trajectory Monte Carlo technique were found to be in excellent agreement with measured spectra at small ejection angles. On the other hand, appreciable discrepancies were observed at large ejection angles for low electron energies, where the calculated cross sections underestimate the magnitude of the experimental data.

In addition to this, total electron yields obtained by integration of the measured doubly differential cross sections and from coincidence measurements of the total ion yields were observed to be approximately 20–30 % larger than the present CTMC calculations.

Further comparison between theory and experiment regarding collisions of clothed ions with atoms would be benefitted, for example, by the investigation of the electron spectra in coincidence with the final charge state of both the target and projectile and with a number of different incident charge states. With particular concern to theory, inclusion of the explicit interactions between target electrons and projectile electrons could result in an enhancement of the ionization cross sections since at these collision velocities the projectile electrons have sufficient mean kinetic energies to ionize the target.[54]

ACKNOWLEDGMENTS

The authors would like to thank Marvin Lien and Mark Middendorf for their support in the operation of the accelerator at Pacific Northwest Laboratory. Marvin Lien also provided software support for analysis of the extensive data generated by these experiments. This work was supported by the Office of Health and Environmental Research (OHER), U. S. Department of Energy, under Contract No. DE-AC06-76RLO 1830, and by the Office of Fusion Energy, U. S. Department of Energy.

[1]H. Toburen, Scanning Electron Microscopy (to be published); in *Nuclear Methods Monograph Series,* edited by D. Berényi and G. Hoch (Elsevier, New York, 1982), Vol. 2, pp. 53–82.
[2]D. Berényi, Vacuum **37**, 53 (1987).
[3]N. Stolterfoht, in *Structure and Collisions of Ions and Atoms,* Vol. 5 of *Topics in Current Physics,* edited by I. A. Sellin (Springer-Verlag, New York, 1978), pp. 155–199.
[4]M. E. Rudd, Radiat. Res. **64**, 153 (1975).
[5]M. Inokuti, Rev. Mod. Phys. **43**, 297 (1971).
[6]S. T. Manson, L. H. Toburen, D. H. Madison, and N. Stolterfoht, Phys. Rev. A **12**, 60 (1975).
[7]N. Stolterfoht, D. Schneider, J. Tanis, H. Altevogt, A. Salin, P. D. Fainstein, R. Rivarola, J. P. Grandin, J. J. N. Scheuer, S. Andriamonje, D. Bertault, and J. F. Chemin, Europhys. Lett. **4**, 899 (1987).
[8]D. S. F. Crothers and J. F. McCann, J. Phys. B **16**, 508 (1983).
[9]P. D. Fainstein, V. H. Ponce, and R. D. Rivarola, J. Phys. B **21**, 287 (1988); **22**, 1207 (1989).
[10]C. R. Garibotti and J. E. Miraglia, Phys. Rev. A **21**, 572 (1980).
[11]R. E. Olson, T. J. Gay, H. G. Berry, E. B. Hale, and V. D. Irby, Phys. Rev. Lett. **59**, 36 (1987).
[12]C. O. Reinhold and R. E. Olson, Phys. Rev. A. **39**, 3861 (1989).
[13]M. E. Rudd, T. Jorgensen, and D. J. Volz, Phys. Rev. **151**, 28 (1966).
[14]R. K. Cacak and T. Jorgensen, Phys. Rev. A **2**, 1322 (1970).
[15]W. E. Wilson and L. H. Toburen, Phys. Rev. A **7**, 1535 (1973).
[16]D. Burch, H. Wieman, and W. B. Ingalls, Phys. Rev. Lett. **30**, 823 (1973).
[17]N. Stolterfoht, D. Schneider, D. Burch, H. Wieman, and J. S. Risley, Phys. Rev. Lett. **33**, 59 (1974).
[18]S. T. Manson and L. H. Toburen, Phys. Rev. Lett. **46**, 529 (1981).
[19]J. H. McGuire, N. Stolterfoht, and P. R. Simony, Phys. Rev. A **24**, 97 (1981).
[20]R. D. DuBois and S. T. Manson, Phys. Rev. Lett. **57**, 1130 (1986); in *Abstracts of Contributed Papers, Proceedings of the Sixteenth International Conference on the Physics of Electronic and Atomic Collisions,* AIP Conf. Proc. No. 205, edited by A. Dalgarno, R. S. Freund, M. S. Lubell, and T. B. Lucatorto (AIP, New York, 1990), p. 432.
[21]P. H. Woerlee, Yu. S. Gordeev, H. de Waard, and F. Saris, J. Phys. B **14**, 527 (1981).
[22]Yu. S. Gordeev and A. N. Zinoviev, in *Physics of Electronic and Atomic Collisions,* edited by S. Datz (North-Holland, Amsterdam, 1982), pp. 169–177.
[23]L. H. Toburen, in *Abstracts of Contributed Papers, Proceedings of the Eleventh International Conference on the Physics of Electronic and Atomic Collisions, Kyoto, 1979,* edited by K. Takayanagi and N. Oda (North-Holland, Amsterdam, 1979), p. 630.
[24]J. M. Hansteen and O. P. Mosebekk, Phys. Rev. Lett. **29**, 1361 (1972); J. H. McGuire and L. Weaver, Phys. Rev. A **16**, 41 (1977).
[25]T. L. Criswell, L. H. Toburen, and M. E. Rudd, Phys. Rev. A **16**, 508 (1977).
[26]L. H. Toburen, Phys. Rev. A **3**, 216 (1971).
[27]M. E. Rudd, L. H. Toburen, and N. Stolterfoht, At. Data Nucl. Data Tables **18**, 413 (1976).
[28]R. D. DuBois, Phys. Rev. A **39**, 4440 (1989).
[29]R. D. DuBois and A. Kover, Phys. Rev. A **40**, 3605 (1989).
[30]R. L. Watson and L. H. Toburen, Phys. Rev. A **7**, 1853 (1973).
[31]N. Stolterfoht, D. Schneider, and K. G. Harrison, Phys. Rev. A **8**, 2363 (1973).
[32]N. Stolterfoht and D. Schneider, Phys. Rev. A **11**, 721 (1975).
[33]N. Kobayashi, N. Maeda, H. Hori, and M. Sakisaka, J. Phys. Soc. Jpn. **40**, 1421 (1976).
[34]A. Langenberg and J. van Eck, J. Phys. B **9**, 2421 (1976).
[35]K. G. Harrison, H. Tawara, and F. J. de Heer, Physica **66**, 16 (1973).
[36]E. Hartmann, J. Phys. B **21**, 1173 (1988).
[37]R. Abrines and I. C. Percival, Proc. Phys. Soc. London **88**, 861 (1966).
[38]R. E. Olson and A. Salop, Phys. Rev. A **16**, 531 (1977).
[39]T. F. M. Bonsen and D. Banks, J. Phys. B **4**, 706 (1971).
[40]R. E. Olson, Phys. Rev. A **18**, 2464 (1978).
[41]R. E. Olson, in *Electronic and Atomic Collisions,* edited by H. B. Gilbody, W. R. Newell, F. H. Read, and C. H. Smith (Elsevier, Amsterdam, 1988), p. 271.
[42]M. R. C. McDowell and R. K. Janev, J. Phys. B **17**, 2295 (1984); R. K. Janev and M. R. C. McDowell, Phys. Lett. **102A**, 405 (1984).
[43]C. O. Reinhold and D. R. Schultz, J. Phys. B **22**, L565 (1989); Phys. Rev. A **40**, 7373 (1989).
[44]G. Peach, S. L. Willis, and M. R. C. McDowell, J. Phys. B **18**, 3921 (1985).
[45]C. O. Reinhold and C. A. Falcón, Phys. Rev. A **33**, 3859 (1986).
[46]J. S. Cohen and G. Fiorentini, Phys. Rev. A **33**, 1590 (1986).
[47]V. J. Montemayor and G. Schiwietz, J. Phys. B **22**, 2555 (1989); Phys. Rev. A **40**, 6223 (1989).
[48]D. Schneider, D. DeWitt, A. S. Schlachter, R. E. Olson, W. G. Graham, J. R. Mowat, R. D. DuBois, D. H. Loyd, V. J. Montemayor, and G. Schiwietz, Phys. Rev. A **40**, 2971 (1989).
[49]R. H. Garvey, C. H. Jackman, and A. E. S. Green, Phys. Rev. A **12**, 1144 (1975).
[50]D. R. Schultz, C. O. Reinhold, and R. E. Olson, Phys. Rev. A **40**, 4947 (1989).
[51]C. O. Reinhold, D. R. Schultz, R. E. Olson, L. H. Toburen, and R. D. DuBois, J. Phys. B **23**, L297 (1990).
[52]R. D. DuBois and L. H. Toburen, Phys. Rev. A **38**, 3960 (1988).
[53]R. K. Janev, R. A. Phaneuf, and H. T. Hunter, At. Data Nucl. Data Tables **40**, 249 (1988).
[54]H. -P. Hulskotter, W. E. Meyerhof, E. Dillard, and N. Guardala, Phys. Rev. Lett. **63**, 1938 (1989).